The International Journal of Advanced Manufacturing Technology (2019) 103:1621–1631
https://doi.org/10.1007/s00170-019-03730-1

ORIGINAL ARTICLE

Structure design and effects of conical gear roller on restraining rabbit ear defects during gear rolling

Tao Wu[1] · Guangchun Wang[1] · Jin Li[2] · Ke Yan[1]

Received: 16 December 2018 / Accepted: 11 April 2019 / Published online: 27 April 2019

Abstract
The gear rolling process using a conical gear roller was developed recently and has been proved to be feasible for forming cylindrical gears. However, the rabbit ear defect, which is normally present in the traditional rolling process, still exists. Therefore, an innovative structure for the conical gear roller is proposed to prevent rabbit ear defects. The size of the dedendum circle during the tooth forming stage is determined according to the height of the growing tooth on the blank at each moment, and the volume of the roller pressed into the blank is equivalent to that of the objective gear's tooth space. Both simulations and experiments are carried out to investigate the effects of the revised rollers on the rolling process. The results show that the formation of the tooth profiles can be effectively confined to the desired volume cavity, so that there is no extra space for the formation of rabbit ears. The tooth is fully filled, and the rabbit ear defects are obviously reduced. The experimental results agree well with the numerical simulation. The present study can help in improving the integrity and accuracy of the formed teeth for the gear rolling process.

Keywords Gear rolling · Conical roller · Structure design · Rabbit ear

1 Introduction

The production of gears in practical industries is dominated by the cutting process, which results in the wastage of significant amounts of material. The rolling process has attracted considerable attention from researchers, as a precision plastic forming method. During the rolling process, the blank is applied a certain amount of force by the rack roller or gear roller at room temperature. The material on the blank surface experiences plastic deformation, and a tooth profile is gradually formed due to the generation of motion between the blank and the roller. Small module gears ($m < 3$) with five-stage precision can be obtained from low tensile strength materials using the cold rolling process, as reported [1]. Compared with the traditional cutting method, the gears formed by rolling have better performance in terms of mechanical properties. Moreover, the material utilization is also much higher in the rolling process.

The forming accuracy of the tooth profile is always a research hotspot in the rolling process for spline or gear parts. Zhang et al. [2–4] studied the deformation characteristic of thread and spline synchronous rolling process and analyzed the influence of phase characteristic between dies on tooth forming accuracy. In the gear rolling process, rabbit ear is a serious defect which needs to be eliminated. Rabbit ear refers to a tip on the tooth corner of the formed gear, as shown in Fig. 1. It is caused by different flow rates of the materials on the surface and inside of the blank. Various methods for improving the forming accuracy in the gear rolling process have been studied through experiments and numerical simulations. Neugebauer et al. [5–8] established a simulation model for gear rolling and proposed a various pitch method to improve the forming accuracy of the tooth profile by 50%. Sasaki et al. [1] developed a rolling machine based on computerized numerical control (CNC) and obtained high-precision helical gears corresponding to DIN 5 through a trial and error method. Khodaee and Melander [9] studied the effects of reversal cycles on the gear rolling process using the FEM method and

✉ Guangchun Wang
wgc@sdu.edu.cn

[1] Key Laboratory for Liquid-Solid Structural Evolution and Processing of Materials (Ministry of Education), Shandong University, Jinan 250061, Shandong, People's Republic of China

[2] School of Mechanical and Electrical Engineering, Shandong Jianzhu University, Jinan 250101, Shandong, People's Republic of China

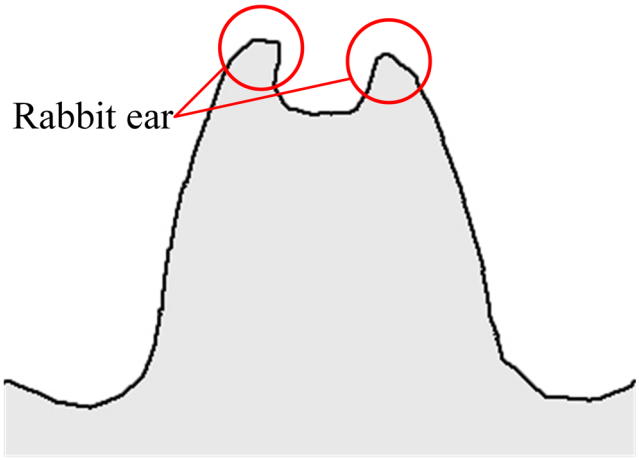

Fig. 1 Rabbit ear defect

evaluated the dimension accuracy of the gear. Li et al. [10] investigated the factors affecting the slippage defect and forming accuracy. Ma et al. [11] presented an analytical model for predicting the pitch error at the initial stage of the gear rolling process.

A novel gear rolling process was proposed in our recent study [12]. Unlike the traditional method, a gear roller with various tooth profiles along the axial direction (we called it conical gear roller) was applied. Moreover, the blank was fed along the axial direction instead of feeding the roller along the radial direction, as indicated in Fig. 2. In the rolling process, the distance between the axis of the rollers and the blank is kept unchanged. The blank is fed to the rollers in the axial direction. After performing continuous rolling in different stages, the outer part of the blank forms the objective tooth profile when the blank departs from the roller. This novel process has been proved to be feasible through numerical simulations and experiments. It not only meets the variable pitch requirements in tooth forming but also has the advantages of uniformity of tooth graduation. However, the widely appearing rabbit ear defect still exists in the process.

Therefore, in order to restrain the rabbit ear defect, we attempt to optimize the structure of the conical gear roller in this study. The dedendum of the roller in the tooth forming stage is modified according to the tooth height during the tooth growing process. The design principle is to make the volume of the roller's tooth space equal to that of the growing tooth of the blank. This ensures that the outer profile of the growing tooth can be enveloped by the dedendum and the flank of the roller's teeth at all times. In addition, the effects of the conical roller with improved structure on the gear rolling process are studied experimentally and numerically. The results show that the teeth of the objective gear were fully filled and that the rabbit ear defect was effectively restrained.

2 Design of conical gear roller

The formation of rabbit ear can be explained by analyzing the force exerted on the growing tooth of the blank. As is seen from Fig. 3, during a single rolling process, tooth C is mainly subjected to the normal pressure and shear friction coming from tooth A and tooth B of the roller. The materials on the blank experience plastic deformation with the generation motion. The deformation mainly occurs on the blank surface which contacts with the roller, and it leads to the fact that the materials simultaneously flow to the top and bottom along the flank of roller. Obviously, the materials are easier to flow to the top since there is enough space. Therefore, a sharp tip is formed at the tooth corner, and the tip gradually accumulates and forms a rabbit ear.

Li et al. [13] and Wang et al. [14] also discussed the mechanism of formation of the rabbit ear in detail. Further, Li et al.

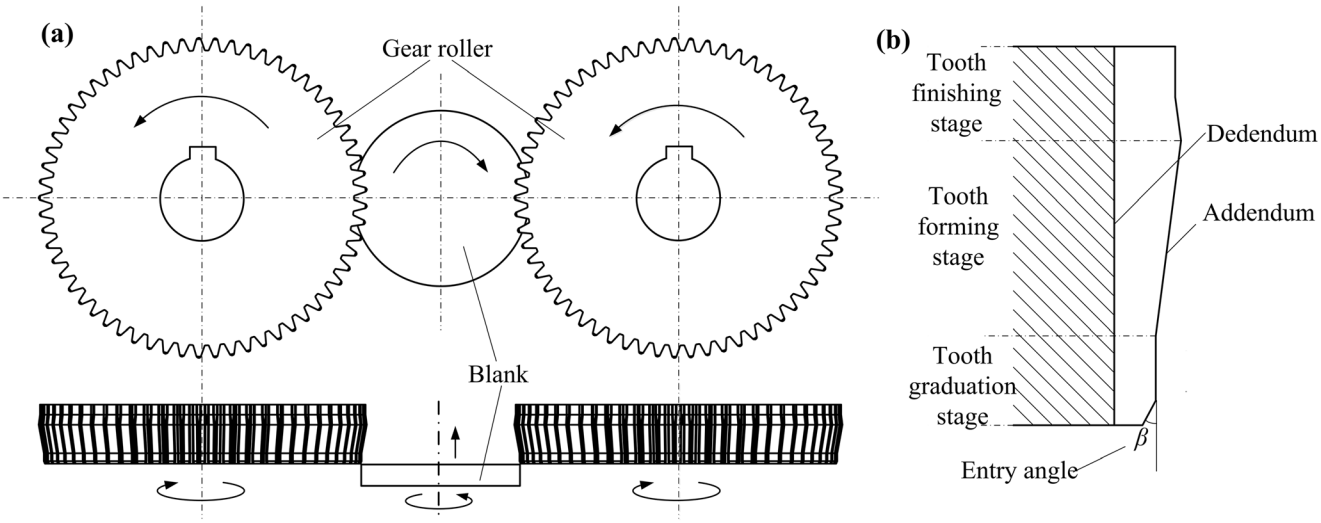

Fig. 2 Schematic diagrams of **a** conical gear rolling and **b** single tooth's structure along the axial direction

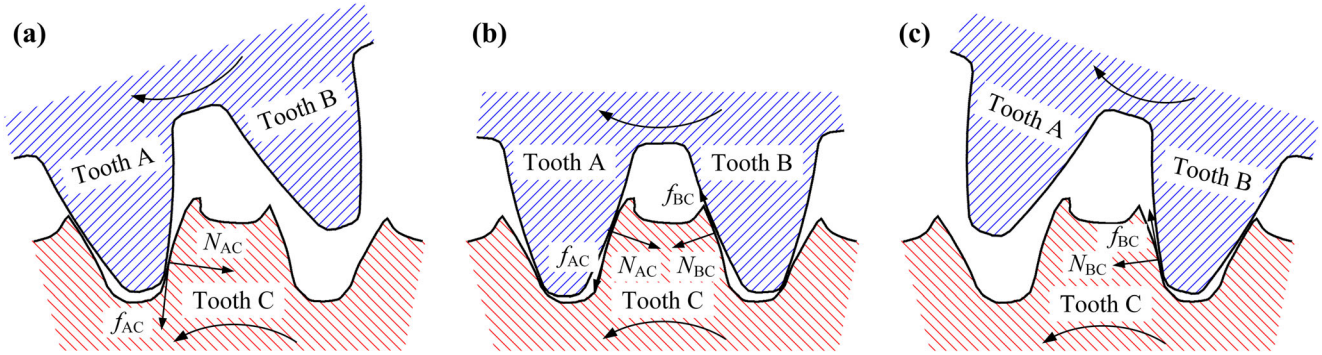

Fig. 3 Force analysis of a tooth growing process in the **a** initial stage, **b** middle stage, and **c** final stage

[15, 16] studied the effect of process parameters on rabbit ear defects and proposed some approaches to reduce the rabbit ear. Fu et al. [17] investigated the large-diameter gear rolling process with a local induction heating method and reduced the rabbit ear defect. Ma et al. [18] designed a rolling tool using an axial feed method and demonstrated that the positive addendum modification on the roller could reduce the height of the rabbit ear. However, the rabbit ear has not been completely eliminated in the above open literatures. Actually, the rabbit ear cannot be completely avoided only by optimizing the process parameters or modifying the roller's addendum structure. Hence, Li [19] proposed a method of decreasing the rabbit ear by restraining the growth of the tooth, as shown in Fig. 4. During the rolling process, a cylindrical roller exerts pressure on the tooth top of the blank. The roller gradually moves backward along the radial direction with the growth of the tooth. However, some problems still exist in the application of this method. Firstly, it is difficult to ensure that the moving speed of the roller is always consistent with the tooth growth speed. Secondly, it is impossible to restrain the flow of materials to the end faces since there is no axial constraint.

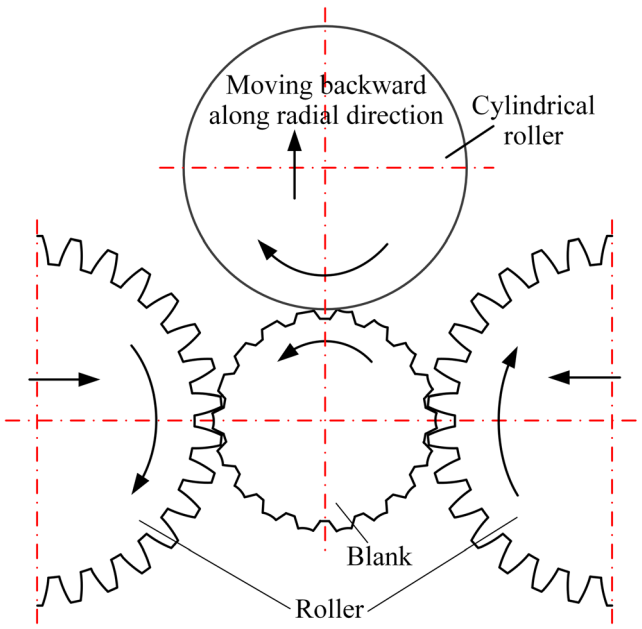

Fig. 4 Schematic diagram of reducing rabbit ear by setting a cylindrical roller on the tooth

In this paper, a method of controlling the tooth growth is adopted to restrain the rabbit ear. Based on the geometry of the previously designed conical roller [12], the roller dedendum in the tooth forming stage was modified. The module of the objective gear is 1 mm, and the tooth numbers of the roller and objective gear are 61 and 31, respectively. The detailed parameters of the previously designed conical roller are given in Table 1 [12] and Fig. 5.

During the gear rolling process, the volume of the roller pressed into the blank is equivalent to that of the objective gear's tooth space. In addition, the growing tooth of the objective gear squeezes into the tooth space of the roller. The enclosed volume of the tooth space can be adjusted by changing the dedendum position of the gear roller. If this enclosed volume is exactly equal to the volume of the growing tooth, the formation of the rabbit ear can be restricted.

From Fig. 5, the formula for calculating the radius of the dedendum circle r_f is expressed as

$$r_f = a - r_z - h_j \quad (1)$$

Table 1 Parameters of the previously designed conical roller

Parameters	Value
Tooth number, z_0	61
Module, m	1 mm
Radius of the dedendum circle, r_f	29.25 mm
Radius of the addendum circle in the tooth graduation stage, r_{a2}	30.75 mm
Radius of the addendum circle at heel in the tooth forming stage, r_{a1}	31.75 mm
Tip radius at heel in the tooth forming stage, r_c	0.4 mm
Pitch Pressure angle at heel in the tooth forming stage, α_0	19.75°
Cone angle of the gear roller in the tooth forming stage, μ	10°
Length of gear roller in the tooth forming stage, l	5.67 mm

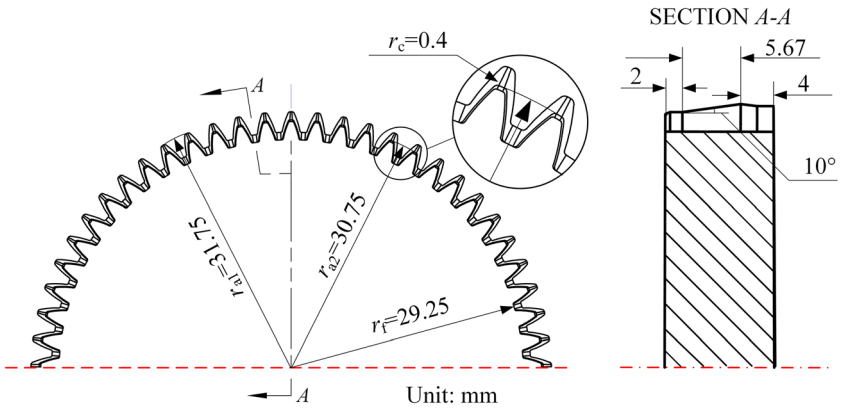

Fig. 5 Geometry of the previously designed conical rollers

where r_f is the radius of the gear roller's dedendum circle, a is the distance between the axial center of the gear roller and the blank, r_z is the radius of the blank, and h_j is the height of the growing tooth.

The relation between the height of the growing tooth h_j and the axial feed of the blank in the forming stage f can be expressed as $h_j = \varphi(f)$. When the blank is fed to the conical gear roller in the tooth forming stage, the volume of the roller-in-blank is equal to that of the growing tooth. Thus, the value of h_j can be obtained.

For simplifying the calculation, the geometry of the model is assumed as follows: (1) There is no fillet on the tooth of the gear roller and the objective gear. (2) The feed during the entire process is regarded as radial feed in order to easily find the relation between the material growth occurring on the blank and the material extruded by the roller. (3) The material flow in axial direction is ignored, and the process is considered as plane deformation. Hence, the diameter of the ideal dedendum circle can be calculated by establishing the formula for area equivalence relation between the materials grown and the materials extruded at any cross section during the entire tooth forming stage.

The area of roller-in-blank S_{roller} can be divided into two parts. The first one is S_{ABCD}, which is enclosed by the dedendum circle, base circle, and tooth profile of the objective gear. The second one is S_{CDEF}, which is outside the base circle of the objective gear. The schematic of these two parts is shown in Fig. 6.

The formula for calculating the tooth thickness on any circle of the involute gear is

$$\begin{cases} s_k = \dfrac{r_k}{r} s - 2r_k(inv\alpha_k - inv\alpha) \\ inv\alpha_k = \tan\alpha_k - \alpha \\ \alpha_k = \arccos\dfrac{r_b}{r_k} \end{cases} \tag{2}$$

where s_k is the tooth thickness on any circle of the involute gear, s is the tooth thickness on the reference circle, r_k is the radius of any circle on the involute gear, α_k is the pressure angle at any point on the involute gear, and α is the pressure angle in the reference circle.

The tooth thickness on the base circle of the objective gear s_b is

$$s_b = \frac{1}{2} m\pi\cos\alpha + mz\cos\alpha inv\alpha \tag{3}$$

where z is the tooth number of the objective gear and m is the module.

Therefore, the tooth space thickness on the base circle of the objective gear s_b' and its center angle φ'_b is

$$s_b' = \frac{2\pi r_b}{z} - s_b = \frac{\pi mz\cos\alpha}{z} - s_b$$

$$= \frac{1}{2}\pi m\cos\alpha - mz\cos\alpha inv\alpha \tag{4}$$

$$\varphi_b' = \frac{s_b'}{r_b} = \frac{\pi - 2z inv\alpha}{z} \tag{5}$$

where r_b is the base radius of the objective gear.

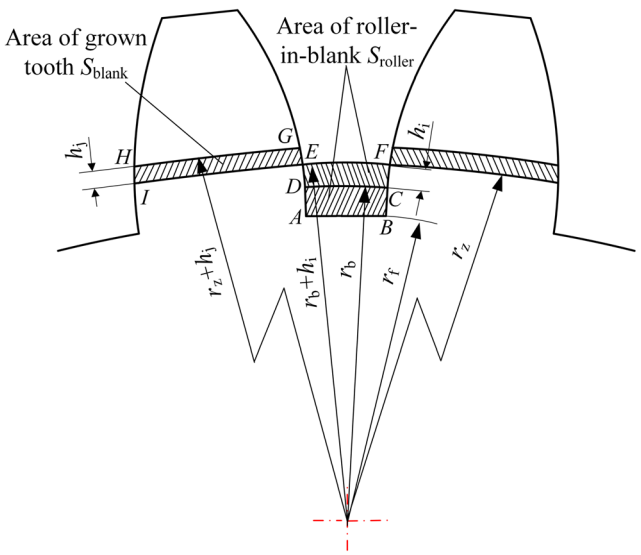

Fig. 6 Schematic diagram for calculating the grown tooth h_j during the rolling process

Table 2 Growing tooth h_j and radius of the roller's dedendum circle r_f at several discrete axial feed positions

Position number	P1	P2	P3	P4	P5
Axial feed, f (mm)	1.134	2.268	3.403	4.537	5.671
Height of growing tooth, h_j (mm)	0.33	0.47	0.63	0.83	1.10
Radius of roller's dedendum circle, r_f (mm)	30.27	30.13	29.97	29.77	29.50

Therefore, S_{ABCD} can be calculated using the following equation:

$$S_{ABCD} = \frac{\pi - 2z inv\alpha}{2z}\left(r_b^2 - r_f^2\right) \tag{6}$$

where r_f is the radius of the dedendum circle of the objective gear.

The area S_{CDEF} outside the base circle can be calculated by following equation:

$$\begin{aligned} S_{CDEF} &= \int_{r_b}^{r_b+h_i}\left(\frac{2\pi r_i}{z} - s_i\right)dr_i \\ &= \int_{r_b}^{r_b+h_i}\left(\frac{2\pi r_i}{z} - \frac{r_i}{r}s + 2r_i inv\alpha_i - 2r_i inv\alpha\right)dr_i \\ &= \int_{r_b}^{r_b+h_i}\left[\frac{2\pi r_i}{z} - \frac{r_i}{r}s + 2r_i inv\left(\arccos\frac{r_b}{r_i}\right) - 2r_i inv\alpha\right]dr_i \end{aligned} \tag{7}$$

where h_i is the distance of the roller-in-blank outside the base circle.

Thus, the formula for calculating the total area of the roller-in-blank S_{roller} can be obtained as follows:

$$\begin{aligned} S_{roller} = S_{ABCD} + S_{CDEF} \quad &= \frac{\pi - 2z inv\alpha}{2z} + \int_{r_b}^{r_b+h_i} \\ &\left[\frac{2\pi r_i}{z} - \frac{r_i}{r}s + 2r_i inv\left(\arccos\frac{r_b}{r_i}\right) - 2r_i inv\alpha\right]dr_i \end{aligned} \tag{8}$$

With the gear roller rolling into the blank, the materials on the outer circle of the blank gradually grow to form a complete tooth. The area of the growing tooth S_{blank} can be calculated by the following equation:

$$\begin{aligned} S_{blank} &= \int_{r_z}^{r_z+h_j}\left(\frac{r_i}{r}s - 2r_i inv\alpha_i + 2r_i inv\alpha\right)dr_i \\ &= \int_{r_z}^{r_z+h_j}\left[\frac{r_i}{r}s - 2r_i inv\left(\arccos\frac{r_b}{r_i}\right) + 2r_i inv\alpha\right]dr_i \end{aligned} \tag{9}$$

According to the relation among the axial feed distance, radial feed distance, and cone angle [12], the distance of the roller-in-blank outside the base circle h_i can be expressed as

$$h_i = 0.835\frac{f}{\tan 10^\circ}, x \in \left[0, \tan 10^\circ\right] \tag{10}$$

By combining Eqs. (8), (9), and (10), the relation between the height of the growing tooth h_j and axial feed distance f in the tooth forming stage can be obtained as follows:

$$h_j = \varphi(f) \tag{11}$$

Since Eq. (11) is a complicated function equation, the value of h_j can be calculated using MATLAB. Thus, the radius of dedendum circle of the roller can be obtained according to Eq. (1).

Table 2 gives the growing tooth h_j and the dedendum circle of the roller r_f at several discrete axial feed positions. Figure 7 shows the curve of the dedendum circle based on Eqs. (1) and (11).

As is seen from Fig. 7, the dedendum circle of the roller decreases rapidly along the axial direction, and it is consistent with the trend of the tooth growth. The radius of the dedendum circle in the tooth graduation section is adjusted to be 30.40 mm in order to permit tooth growth in this stage. In addition, a fillet is set at the junction of the tooth forming and finishing stages. Figure 8 shows the dedendum of the roller before and after revision.

3 Numerical simulations

To verify the effects of the revised conical gear roller, numerical simulation of the rolling process was carried out using DEFORM-3D. According to the equal volume principle, the radius of the blank r_z is calculated as 15.4 mm. In order to enhance the simulation efficiency, a blank with a half-circular shape is utilized, and the thickness is chosen as 0.5 mm. Since the rolling process is a cold forming process, pure aluminum

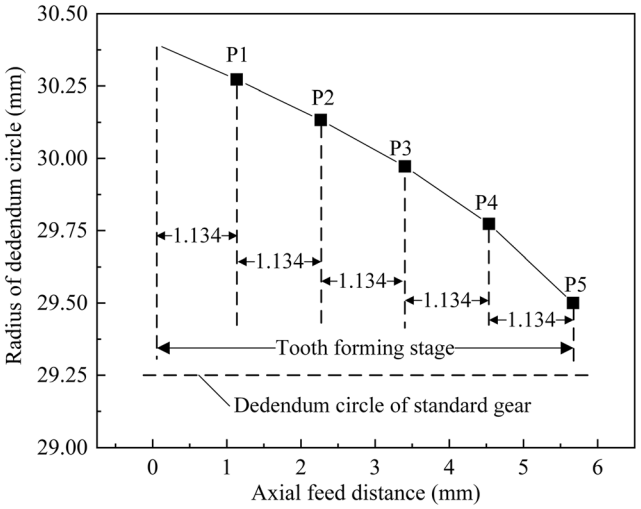

Fig. 7 Variation diagram of the revised dedendum cycle's radius

with good plasticity is selected as the blank material. To prevent blank eccentricity, the motion relationship between the blank and roller is set as follows. The blank is kept fixed, while the roller is rotated and fed. Moreover, the blank's rotation is converted into the gear roller's revolution. The process parameters in the numerical simulation are shown in Table 3. The finite element model of the conical gear rolling process is shown in Fig. 9.

Figures 10 and 11 show the simulated results for the velocity fields of the blank using the revised and unrevised rollers, respectively, in the tooth forming stage. As seen in Fig. 10, the space is enveloped by the roller's dedendum, and the tooth flank of the adjacent teeth becomes smaller. The volume of the tooth space is equal to the volume required for the tooth growth. This ensures that the tooth forming process can be confined to the predetermined cavity at each moment. Thus, there is no extra space for the formation of rabbit ear. Although the materials at the tooth top have an upward flow tendency, they are prevented by the dedendum of the rollers. However, this is not the case when using the unrevised rollers, as shown in Fig. 11. The rabbit ear appears from the beginning and increases gradually during the entire forming stage.

After the completion of the tooth forming stage, the tooth morphology using the revised and unrevised rollers is obtained as shown in Fig. 12. It can be seen that the tooth has been fully filled, and the rabbit ear has almost disappeared when using the revised gear roller.

Figure 13 shows a part of the tooth morphology at the center section plane of the obtained gear after the tooth finishing stage. The section of the conical roller is converted into a standard gear in this stage. It can be seen that the tooth profile is further improved by repeated rolling and meshing with the standard gear. When the blank is away from the rollers, the tooth profile of the obtained gear is very close to that of the standard gear.

In order to evaluate the accuracy of the obtained gear further, the various dimensional parameters shown in Fig. 13 are compared with those of the standard gear. Table 4 lists the average values of the parameters by measuring 15 teeth. The addendum height, dedendum height, tooth thickness, tooth space width, and pitch are based on the theoretical pitch circle of the standard gear. From Table 4, it can be seen that the values of most parameters are almost the same as that of the standard gear. However, compared to the standard gear, the addendum circle is slightly smaller and the dedendum circle is larger, which results in inadequate tooth depth. In the future, the addendum of the conical roller should be improved further.

Table 3 Process parameters of the rolling process in finite element modeling

Parameters	Value
Angular velocity of the gear roller's revolution, ω_{re}	30 rpm
Angular velocity of the gear roller's rotation, ω_{ro}	15.246 rpm
Distance between the axial center of gear roller and blank, a	46 mm
Axial feed speed of the roller, v_r	0.1 mm/s
Friction factor	0.12

4 Experimental verification

An experiment for the conical gear rolling process using revised rollers was carried out using a self-made device to further validate the effect of restraining the rabbit ear defect. A 18Ni300 steel roller was manufactured using 3D printing technology (selective laser melting technology) due to its complicated structure. In addition, the roller was heat-treated to improve its strength after manufacture. As the material for the blank, we selected 1100 aluminum alloy. The thickness of the blank was designed to be 5 mm, and two similar blanks with thicknesses of 3 mm or 4 mm were fixed at both end faces and used as baffles. Due to the limited load capacity of the device, the rotation velocity of the roller was around 10 rpm during the experiment. The other conditions were consistent with that in the simulation. The device and the experimental process are shown in Fig. 14.

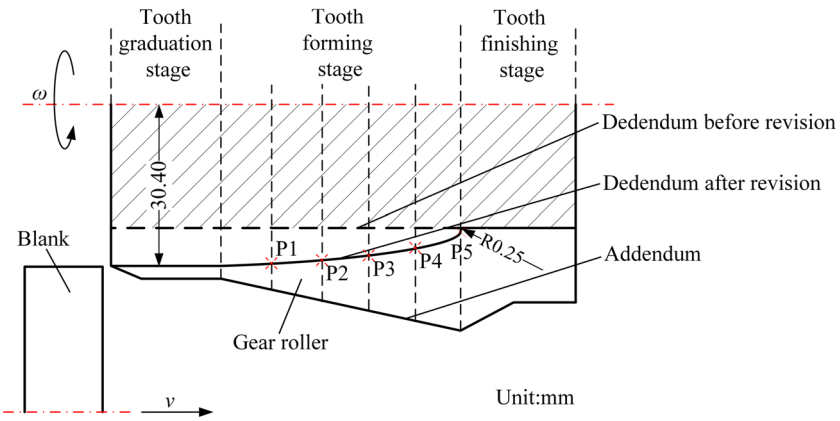

Fig. 8 Schematic diagram of the revised dedendum on the conical gear roller

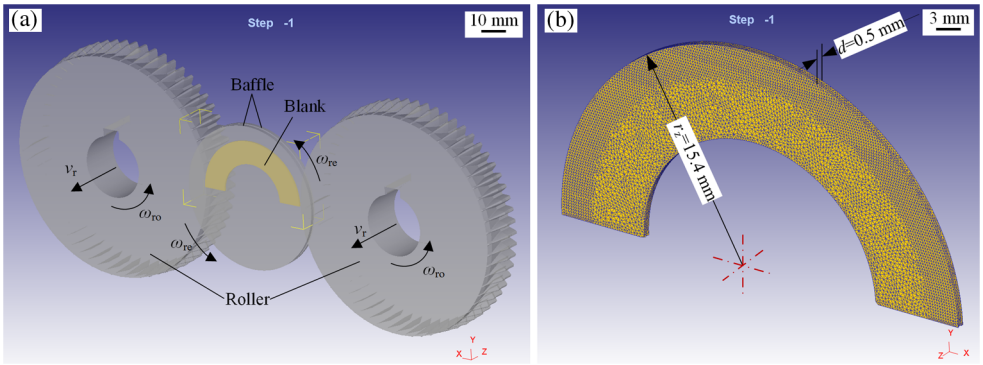

Fig. 9 Finite element modeling of the **a** rolling process and **b** enlarged blank

Figure 15 shows the gear samples obtained after the rolling experiments. As can be seen from the axial view shown in Fig. 15a, the tooth profile of the obtained gear is close to that of the standard gear. Moreover, the obtained gear samples can mesh well with each other. However, although the baffles prevented the axial flow of the material, some material still overflowed to the end face near the forming regions. In Fig. 15a, the top row shows the entrance surface of the sample, while the bottom row shows the exit surface. It is observed that the overflowing phenomenon at the exit face is more serious than that at the entry face. This leads to inadequate tooth width of the obtained gears. From the radial view shown in Fig. 15b, it is seen that the surface quality of the tooth is lower than that obtained when manufactured using the cutting method.

Figure 16 compares the tooth morphology of the gear samples obtained using the revised roller and unrevised roller. Obviously, the rabbit ear does not appear on the tooth produced using the revised roller. This indicates that the revised conical gear roller has successfully restrained the formation of rabbit ear.

Figure 17 shows the tooth profiles obtained by cutting the blank along the radial direction during the feeding process. From Fig. 17, it is seen that the rabbit ear does not appear in the entire duration of the tooth forming stage. It is demonstrated that the forming region of the tooth shape has been confined in the predetermined cavity based on the above calculation and design. It also agrees well with the numerical simulation results.

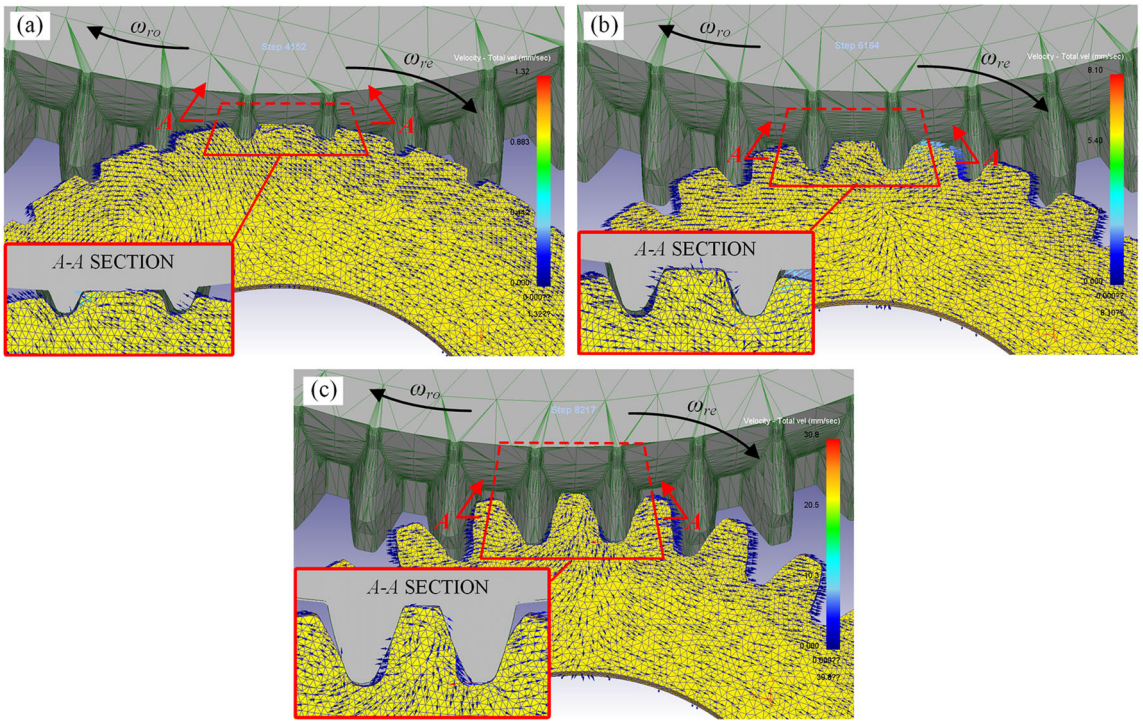

Fig. 10 Velocity field of the blank and tooth formation in the gear rolling process using the revised rollers. **a** One-third feed. **b** Two-third feed. **c** Complete feed

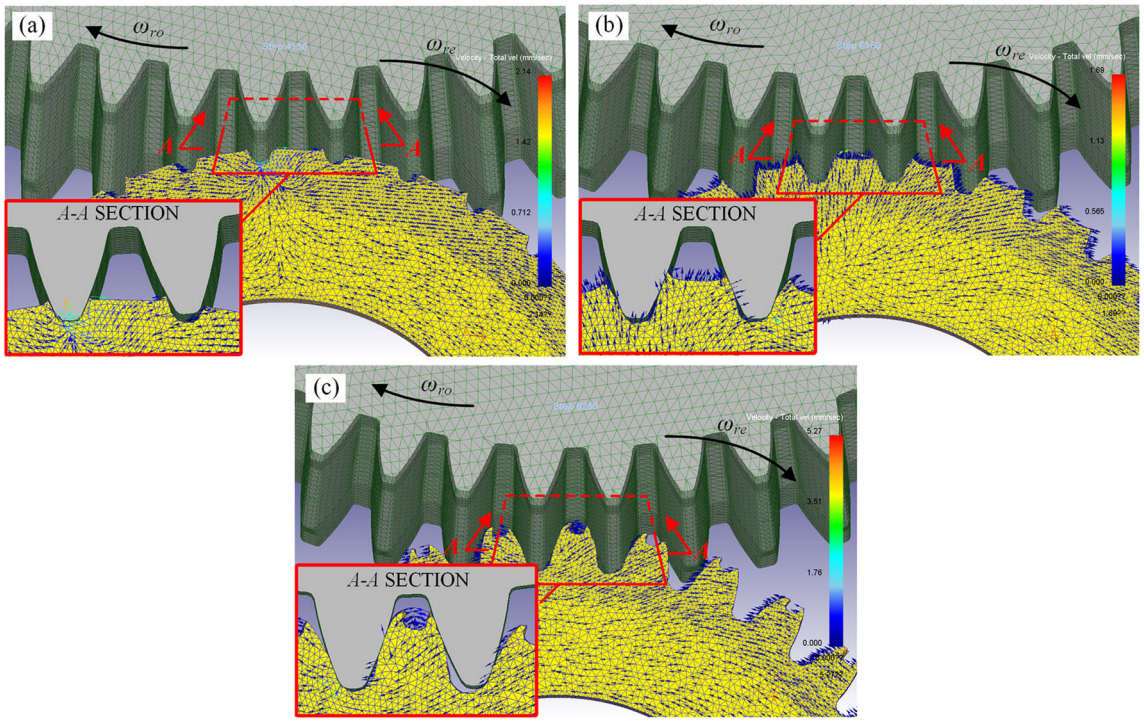

Fig. 11 Velocity field of the blank and tooth formation in the gear rolling process using the unrevised rollers. **a** One-third feed. **b** Two-third feed. **c** Complete feed

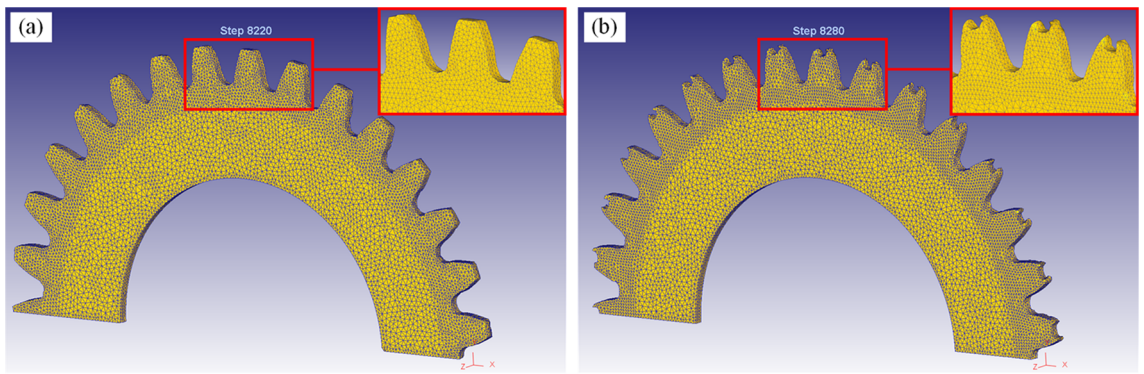

Fig. 12 Tooth morphology at the end of tooth forming stage using **a** revised rollers and **b** unrevised rollers

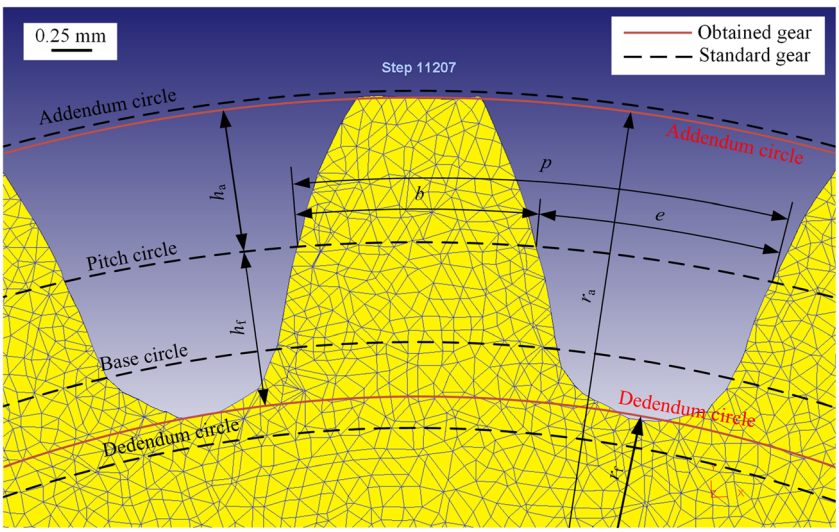

Fig. 13 A part of the tooth morphology at the center section plane of the obtained gear after the tooth finishing stage

Table 4 Parameters of the gear rolled by the revised conical roller and standard gear

Parameters	Obtained gear	Standard gear	Deviation
Radius of addendum circle, r_a (mm)	16.458	16.500	−0.042
Radius of dedendum circle, r_f (mm)	14.437	14.250	+0.187
Addendum height, h_a (mm)	0.958	1.000	−0.042
Dedendum height, h_f (mm)	1.063	1.250	−0.187
Tooth depth, h (mm)	2.021	2.250	−0.229
Tooth thickness, b (mm)	1.577	1.571	+0.006
Tooth space width, e (mm)	1.582	1.571	+0.011
Pitch, p (mm)	3.159	3.142	+0.017

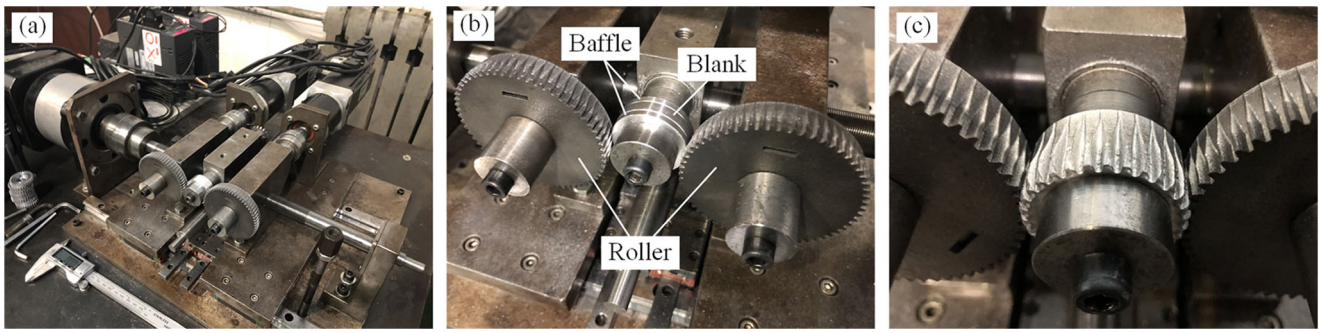

Fig. 14 Photograph of **a** gear rolling device, **b** local enlarged view of the rollers section, and **c** experimental process

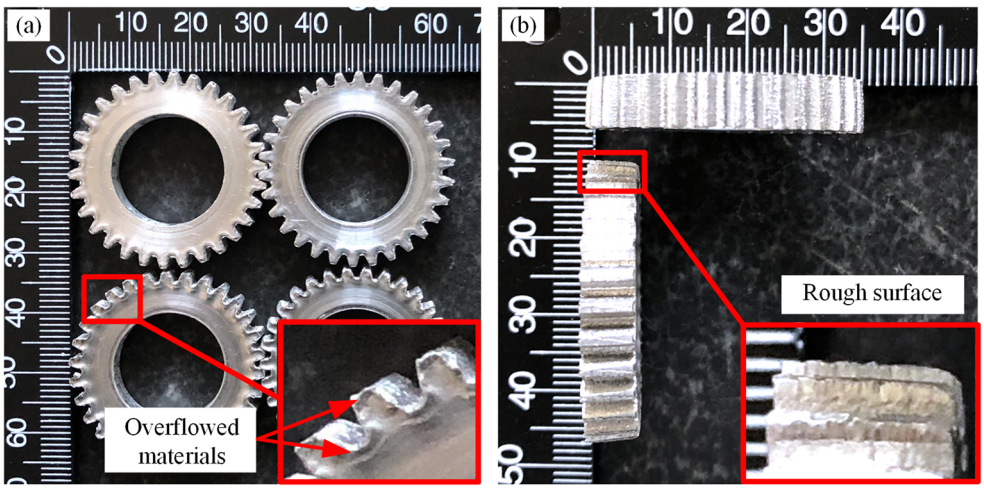

Fig. 15 Obtained gear samples in the **a** axial view and **b** radial view

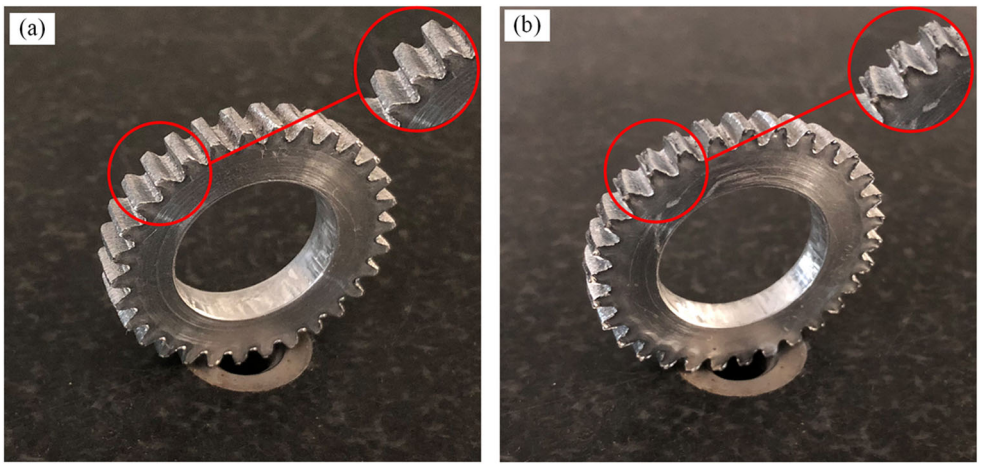

Fig. 16 Tooth morphology on the gear samples obtained by using **a** revised rollers and **b** unrevised rollers

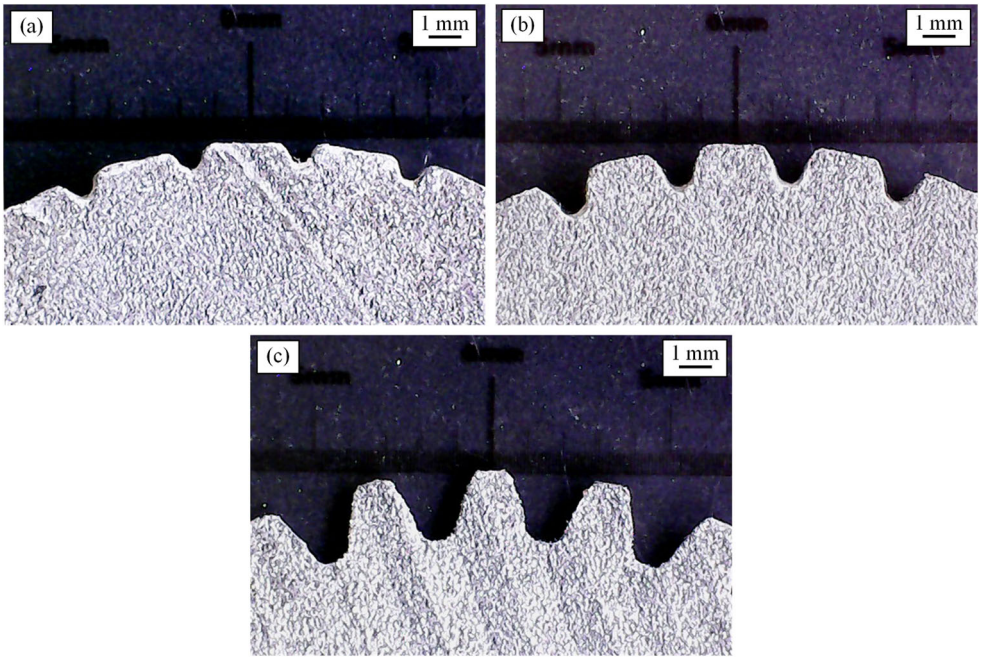

Fig. 17 Tooth profiles at the cross section after radial cutting at **a** one-third feed, **b** two-third feed, and **c** complete feed

5 Conclusions

The rabbit ear is a severe defect, which is difficult to be eliminated in the gear rolling process. In this paper, a revised method for the dedendum of the conical gear roller was proposed to restrain rabbit ear defects. Numerical simulation was conducted to study the effects of the modified rollers on the rolling process, and the simulated results were further verified by performing rolling experiments. The main conclusions are summarized as follows.

(1) By revising the dedendum structure of the conical gear roller, the volume enclosed by roller's tooth flank and dedendum can be accurately adjusted to that required for the tooth growth. Thus, there is no space for the formation of rabbit ear. The detailed formulas to calculate the radius of the dedendum circle are given in the paper.

(2) The simulated results showed that when the revised rollers were used, the tooth formation was confined to the predetermined cavity at each moment. Rabbit ear was not formed during the entire gear rolling process. The obtained gear has a good pitch but inadequate tooth width, which means that the addendum of the conical roller should be improved further.

(3) In the experiments, it is observed that the gears obtained using the revised rollers have a good tooth shape and no rabbit ear. The results prove that the proposed method of revising the roller's dedendum has obvious positive effects on avoiding the rabbit ear defect.

Funding information This work received financial support from the National Natural Science Foundation of China (Grant No. 51475271).

References

1. Sasaki H, Shinbutsu T, Amano S, Takemasu T, Sugimoto S, Koide T, Nishida S (2014) Three-dimensional complex tooth profile generated by surface rolling of sintered steel helical gears using special CNC form rolling machine. Procedia Eng 81:316–321
2. Zhang DW, Zhao SD (2014) New method for forming shaft having thread and spline by rolling with round dies. Int J Adv Manuf Technol 70:1455–1462
3. Zhang DW, Zhao SD, Wu SB, Zhang Q, Fan SQ, Li J (2015) Phase characteristic between dies before rolling for thread and spline synchronous rolling process. Int J Adv Manuf Technol 81:513–528
4. Zhang DW, Zhao SD (2016) Deformation characteristic of thread and spline synchronous rolling process. Int J Adv Manuf Technol 87:835–851
5. Neugebauer R, Putz M, Hellfritzsch U (2007) Improved process design and quality for gear manufacturing with flat and round rolling. CIRP Ann Manuf Technol 56:307–312
6. Neugebauer R, Klug D, Hellfritzsch U (2007) Description of the interaction during gear rolling as a basis for a method for the prognosis of the attainable quality parameters. Prod Eng Res Dev 1: 253–257
7. Neugebauer R, Hellfritzsch U, Lahl M (2008) Advanced process limits by rolling of helical gears. Int J Mater Form 1(1):1183–1186
8. Neugebauer R, Hellfritzsch U, Lahl M, Schiller S, Milbrandt M (2011) Innovations in rolling process of helical gears. AIP Conference Proceedings 1315:569–574
9. Khodaee A, Melander A (2014) A study of the effects of reversal cycle in the gear rolling process by using finite element simulations. Key Eng Mater 611–612(3):134–141

10. Li J, Wang GC, Wu T (2016) Numerical simulation and experimental study of the slippage phenomenon in gear rolling. J Mater Process Technol 234:280–289
11. Ma ZY, Luo YX, Wang YQ (2018) On the pitch error in the initial stage of gear roll-forming with axial-infeed. J Mater Process Technol 252:659–672
12. Wu T, Wang GC, Li J, Yan K (2018) Investigation on gear rolling process using conical gear rollers and design method of the conical gear roller. J Mater Process Technol 259:141–149
13. Li J, Wang GC, Wu T (2017) Numerical-experimental investigation on the rabbit ear formation mechanism in gear rolling. Int J Adv Manuf Technol 91:3551–3559
14. Wang GC, Li J, Wu T (2017) Numerical simulation and experimental investigation on the gear rolling process. Procedia Eng 207:609–614
15. Li J, Wang GC, Wu T (2018) Effect of process factors on the rabbit ear based on numerical simulation and experimental study in gear rolling. Int J Adv Manuf Technol 94:4055–4064
16. Li J, Wang GC, Wu T (2018) Effects of the material and its temperature state on the tooth morphology in gear rolling. Int J Adv Manuf Technol 97:345–352
17. Fu XB, Wang BY, Zhu XX, Tang XF, Ji HC (2017) Numerical and experimental investigations on large-diameter gear rolling with local induction heating process. Int J Adv Manuf Technol 91:1–11
18. Ma ZY, Luo YX, Wang YQ, Mao J (2018) Geometric design of the rolling tool for gear roll-forming process with axial-infeed. J Mater Process Technol 258:67–79
19. Li J (2017) Numerical simulation and experimental research of spur cylindrical gear rolling. Dissertation, Shandong University